ISSN: 2148-6832

MSD Medical Science and Discovery
December 2014, Vol.1, No.4, p:96-108

Original Article Doi: 10.17546/msd.21367

Genotoxicity and Cytotoxicity of novel 10B carrier ((2R)-4,5,6-trihydroxy-2-(hydroxymethyl)tetrahydro-2H-pyran-3-yl)boronic acid

Zafer Akan[1], Hulya Ozdemir[2], Gokhan Oto[2], Sabahattin Deniz[3], Omer Kacar[4], Ali Sadi Basak[5], Tahir Cakır[6], Hatice Uslu Sinav[7], Goksel Demir[8]

Abstract

Objective: Although surgery and chemotherapy have been greatly successful in the treatment of many types of tumors, these treatment modalities have some limitations. In particular, the side effects of conventional radiotherapy warrant the development of new therapy methods, such as Boron Neutron Capture Therapy (BNCT). In the present study, the cytotoxic and genotoxic properties of novel synthesized boron carrier, ((2R)-4,5,6-trihydroxy-2-(hydroxymethyl)tetrahydro-2H-pyran-3-yl)boronic acid (**^{10}**BDG), and the apoptotic pathways triggered by ^{10}BDG were examined.

Material and Methods: As it defined previously, ^{10}BDG was complexed through a low-high pH reaction and was tested using a Fournier Transform InfraRed-Attenuated Total Reflectance (FT-IR/ATR) spectrophotometer. The cytotoxicity of **^{10}**BDG was tested through the MTT assay. The detection of caspases 3, 8, and 9 was performed to determine the activated apoptotic pathways by ^{10}BDG. The Poly (ADP-Ribose) Polymerase (PARP) cleavage and DNA damage induced by this compound were tested through western blot and Terminal deoxynucleotidyl transferase dUTP nick end labeling (TUNEL) assay, respectively.

Results: The average $LogIC_{50}$ and $LogLD_{50}$ levels of ^{10}BDG over NCI-H209 cell line were to be found 72.1±10 µg/ml and 171.8±25 mg/kg, respectively. Caspase-9 activation, caspase-3 activation, PARP cleavage, and caspase-3-dependent DNA fragmentation were observed. The genotoxicity analysis was performed using the plasmid fragmentation assay, which revealed the absence of fragmentation.

Conclusion: Bio-distrubition analysis showed that boron content was elevated to 12.63 from 4.44 ppm in the tumor tissue by the ^{10}BDG injections. In epitome, ^{10}BDG exhibit slight cytotoxic but no genotoxic properties. Based on the antiproliferative properties of ^{10}BDG, in addition to acting as an adjuvant in cancer radiotherapy and chemotherapy, this compound appears to be an alternative boron carrier for BNCT

Keywords: ((2R)-4,5,6-trihydroxy-2-(hydroxymethyl)tetrahydro-2H-pyran-3-yl)boronic, ^{10}BDG, Apoptosis, Genotoxicity, Cancer, BNCT, MAT-LyLu, Biodistribution

Introduction

Boron neutron capture therapy (BNCT) is a type of radiotherapy with the aim of selectively killing cancer cells while reducing the side effects of conventional radiotherapy methods. The procedure of BNCT involves targeting of ^{10}B (15-30 ppm) to tumor tissue, irradiation of ^{10}B with thermal or epithermal neutrons (≤10 KeV; ≈10^9 n^0 sec/cm^2) followed by the release of ^{4}He and ^{7}Li ions in the tumor tissue (see reactions below) [1]. ^{4}He and ^{7}Li are characterized by short ranges in tissue, due to their high linear energy transfer (LET) values. For this reason, tumor tissue may be selectively destroyed by the application of BNCT [2, 3].

$^{10}B+^1n \rightarrow ^7Li$ (0.84 MeV) + ^{4}He (1.47 MeV) + γ (0.48 MeV) 93.7%
$^{10}B+^1n \rightarrow ^7Li$ (1.01 MeV) + ^{4}He (1.78 MeV) 6.3%

The average allowed annual occupational exposure is approximately 50 mSv/year for 18-year-old males and 5 mSv/year for pregnant women [4]. However, the total applied fractional gamma radiation dose can reach 60 Gy during conventional radiotherapy. In high-dose therapy procedures,

Received: 15 Oct. 2014**, Revised** 17 Oct. 2014**, Accepted** 21 Oct. 2014**, Available Online** 25 Oct. 2014
[1]Celal Bayar University School of Medicine, Department of Biophysics 45040 Uncubozkoy Manisa-Turkey
[2]Yuzuncu Yil Universtiy, School of Medicine, Department of Pharmacology, Van-Turkey
[3]Marmara University, Faculty of Technology, Department of Textile Engineering, Istanbul-Turkey
[4]TUBITAK Marmara Research Center, Genetic Engineering and Biotechnology Institute, Gebze-Kocaeli, Turkiye
[5]Marmara University, Faculty of Art&Science, Department of Inorganic Chemistry, Istanbul-Turkey
[6]Yuzuncu Yil University School of Medicine, Department of Radiation Oncology, Van-Turkey
[7]Istanbul Medeniyet University, School of Medicine, Department of Nuclear Medicine, Istanbul-Turkey
[8]Bahcesehir University School of Engineering, Department of Environmental, Istanbul-Turkey
*Corresponding Author: Zafer Akan E-mail: zafer.akan@cbu.edu.tr

exposing healthy tissue adjacent to a tumor site is unavoidable. It is known that X- or Gamma-radiations are absorbed also by healthy tissue and not just tumor tissue during radiotherapy. This unwanted exposure during conventional radiotherapy has side effects on the patients.

In particular, for example the neuroendocrine and cardiovascular systems are susceptible to irreversible damage [5]. Although some precautions, such as the collimation of X and gamma radiation and limited dose calculations, are taken, there is no way to fully protect patients from unwanted exposures. In addition, the energy transfer properties of different radiations are also important. Whereas X- and gamma energies are absorbed by the encountered tissue exponentially with depth, the energy absorption curve of neutron and proton is quite different from that of X and gamma radiation [6]. If all side effects of X and gamma rays and all of the beneficial uses of neutrons are considered, BNCT is hypothesised to be an alternative radiotherapy method particularly for the treatment of head and neck cancers [6]. The most important challenge associated with BNCT is the targeting of ^{10}B to the tumor tissue. At present, different strategies and carriers are being used for carrying ^{10}B to tumor tissue [7, 8, 9].

The glucose analogue 2-deoxy-D-glucose (2-DG) is an inhibitor of glucose transport and glycolytic ATP production. In addition to depleting energy in cells, 2-DG has also been found to alter N-linked glycosylation, which results in unfolded protein responses and the induction of changes in the gene expression and phosphorylation status of proteins involved in signalling, cell cycle control, DNA repair, calcium influx, and apoptosis [10]. It is well known that the glucose metabolism in tumor tissue increases due to, for example, the lack of oxygen, a decreased oxidative phosphorylation, the activation of anaerobic respiration pathway by tumorogenic cells for ATP synthesis, and finally the requirement of excess glucose consumption [11]. Due to the affinity of glucose to tumor tissue, ^{18}F conjugated glucose (^{18}F-Deoxy-D-glucose) is routinely used for the detection and staging of tumors with positron emission tomography (PET). In this technique, ^{18}F-DG releases positrons in the tumor tissue and detectors detect the gamma radiation from electron-positron annihilations [7]

Boric Acid and Deoxy-D-Glucose has been complexed and ^{10}BDG [((2R)-4,5,6-trihydroxy-2-(hydroxymethyl)tetrahydro-2H-pyran-3-yl)boronic acid] synthesized via pH reaction, complexation yield was found about 80% in our previous studies [12]. As extended research, the antineoplastic properties of ^{10}BDG were examined in the present study because it is considered as an alternative ^{10}B carrier for BNCT.

Materials and Methods

Complexation reaction of $B(OH)_3$ and 2-DG

The complexation reaction of boric acid with polyhydroxyl compounds, such as tiron, has been described in previous studies [13]. First, 0.1 M boric acid ($B(OH)_3$; Sigma-Aldrich, B6768) and 0.5 M deoxy-D-glucose (DG: Sigma-Aldrich, D8375) solutions were prepared with the same volumes of deionised water and incubated for one hour at pH 3 and 50°C.

$B(OH)_3 + H_2O \leftrightarrow B(OH)_4^- + H^+$
$Ka= [B(OH)_4^-][H^+] / [B(OH)_3]$

$B(OH)_4^- + DG \leftrightarrow BDG + H^+$
$Ka= [B(OH)_4^-][DG] / [BDG]$

Both solutions were then mixed in the same tube and incubated for one hour at pH 3. The pH was gradually increased from pH 3 to pH 7 and stabilised at a physiologic value of pH 7.4. The $]^{10}BDG$ complexation reaction was tested using a Fourier Transform Infrared Attentuated Total Reflectance spectroscopy (FT-IR/ATR), as previously described (Figs. 1a, 1b, and 1c) [13]. The Accelrys Discovery Studio Visualiser software (version 3.5) was used for the molecular simulations. The synthesized molecule was named according to the International Union of Pure and Applied Chemistry (IUPAC) rules for naming [14, 15].

Name: BDG; ^{10}BDG (Figure 1a);
IUPAC Name: ((2R)-4,5,6-trihydroxy-2-(hydroxymethyl)tetrahydro-2H-pyran-3-yl)boronic acid
BDG molecular weight: 193.953;
exact BDG molecular weight: 194.06;
molecular formula: $C_6H_{11}BO_7$ [15].

Cytotoxicity evaluation of ^{10}BDG on different human cancer cell lines

Due to differences in the cellular structure and function, the cellular response to cytotoxic materials can be different in somatic cell lines. For this reason, in vitro cytotoxicity tests should be applied over the different cell lines before in-vivo application and Lethal Dose 50 ($logLD_{50}$) tests in the experimental animal. For this reason, the cytotoxic levels of the synthesized molecule (^{10}BDG) were tested on different cancer cell lines (HT29 - human colon adenocarcinoma cell line, NCI-H209 - human small cell lung cancer cell line, Raji - Burkitt's Lymphoma, B lymphocyte cell line, and MCF-7 - human breast adenocarcinoma cell line) using the 3-(4,5,dimethylthiazol-2yl)2,5-

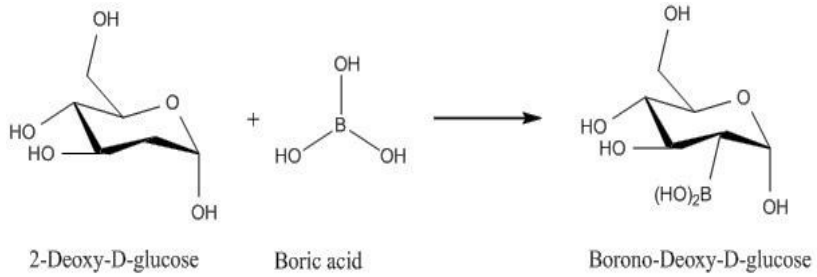

Figure 1a: Representation of (2,4,5,6-tetrahydroxyoxan-3-yl)boronic acid (^{10}BDG).

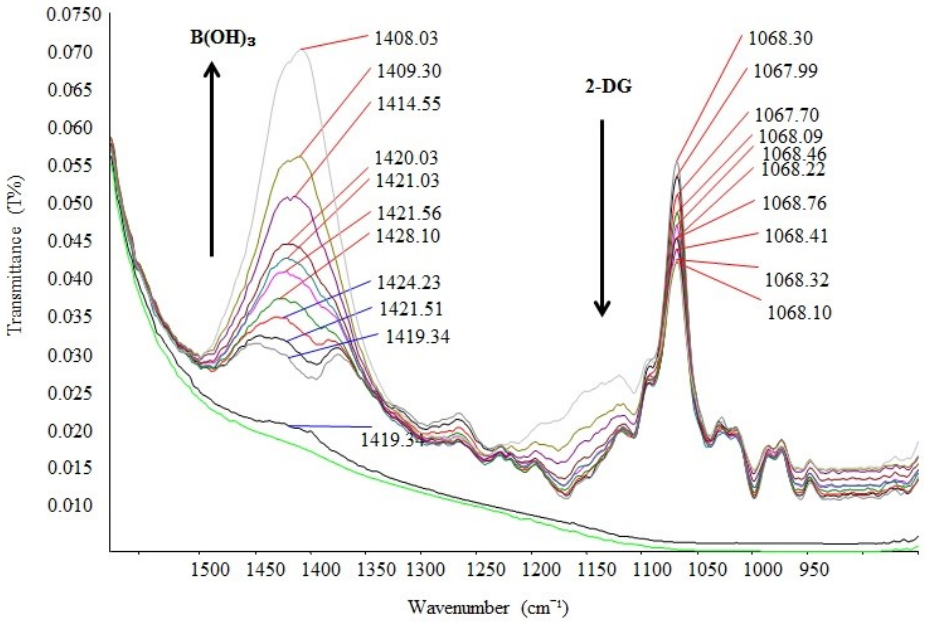

Figure 1b: FT-IR/ATR results of successful complexation of boric acid ($B(OH)_3$) and deoxy-D-glucose (DG). Increased boric acid concentration resulted in a peak shift of deoxy-D-glucose which indicates complexation.

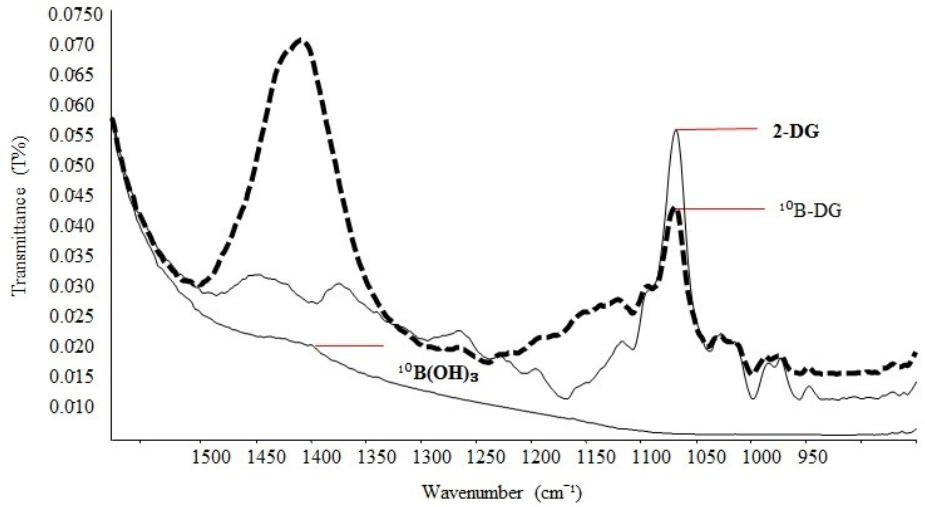

Figure 1c: FT-IR/ATR results of successful complexation of boric acid ($B(OH)_3$) and deoxy-D-glucose (DG). Increased boric acid concentration resulted in a peak shift of deoxy-D-glucose which indicates complexation.

diphenyl tetrazolium bromide (MTT) assay (American Tissue Cell Culture, 30-1010K). All of the cell lines ($3x10^4$ cell/ml) were seeded into a 96-well plate and incubated in a CO_2 incubator at 37°C for 24 hours. Then, ^{10}BDG (0, 10, 20, 40, 80, and 160 µM ^{10}B) was added to the cell suspensions in 100 µl of fresh RPMI-1640 medium (RPMI 1640 R8758-Sigma, 0.5% Pen/Strep, Sigma-Aldrich). After the cell suspensions were incubated with ^{10}BDG for 3 and 24 hours, 1/10 MTT solution was

added to the cells. The cells were then incubated for one hour in a CO_2 incubator. The RPMI medium was removed with a centrifuge, and the purple MTT-formazan crystals were dissolved through the addition of 100 µl of dimethyl sulfoxide (DMSO). The purple color was read at 570 nm using a microplate reader. GraphPad Prism 2 was used for the calculation of the Inhibitory Concentration 50 ($LogIC_{50}$) values. The Lethal Dose 50 ($logLD_{50}$) levels were calculated from the IC_{50} MTT cytotoxicity results according to Interagency Coordinating Committee on the Validation of Alternative Methods (ICCVAM)

The World Health Organization recommends the formula 'Log LD50 (mg/kg) = 0.372 log IC_{50} (µg/mL) + 2.024' to determine the $LogLD_{50}$ value from the $LogIC_{50}$ value, and this should be the first step for testing of the LD_{50} in animal studies [17].

Evaluation of apoptotic pathway triggered by ^{10}BDG for the NCI-H209 cell line

Due to its high metastatic characteristics and its insensitivity to chemotherapy, the NCI-H209 small-cell lung cancer cell line was chosen to triggered pathway analysis by the ^{10}BDG.

To examine the cytotoxic pathways induced by ^{10}BDG, the activities of caspase 9, caspase 8, and caspase 3 were tested with the FAM FLICA active caspase detection reagents (FAM-LEHD-FMK caspase 9, FLICA *FAM*-DEVD-FMK caspase 3, *FAM*-LETD-FMK caspase 8 assay kits, Immunochemistry) using a fluorescence spectrophotometer (Perkin Elmer, EnSpire Multimode Plate Reader Label-free System).

A total of 10^6 NCI-H209 cells were seeded in a 6-well plate and incubated for 24 hours. After the medium was changed, defined concentrations of ^{10}BDG were added in fresh growth medium [RPMI 1640, Hyclone RPMI 1640 with HEPES/L-GLU SH30255 and 1% Pen/Strep solution (Biological Industries, 10,000 U/mL Pen, 10 mg/mL Strep, Kibbutz Beit HaEmek, Israel 25115)]. After three-hour incubation with ^{10}BDG, 10^6 H209 cells were collected and washed with phosphate buffered saline (PBS). The solution of the caspase assay kit was then added to the suspended cells, and the samples were incubated for 30 minutes in a CO_2 incubator at 37°C. The cells were collected and washed three times with 1X apoptosis wash buffer according to the protocol recommended by the kit's manufacturer, and analyzed using a fluorescence plate reader (Perkin Elmer, EnSpire Multimode Plate Reader Label-free System).

PARP cleavage examination of the NCI-H209 cell line

The PARP cleavage was tested with a western blot analysis. First, 10^6 NCI-H209 small cell lung cancer cells (ATCC® HTB-172™) were incubated with ^{10}BDG solution in growth medium (RPMI 1640 R8758-Sigma, 10% FCS, 0.5% Pen/Strep, Sigma-Aldrich). The cells were collected after three hours and washed with PBS. The cells were then lysed with 100 µl of lysis buffer (25 mM Tris-HCl pH 7.4, 150 mM NaCl, 1% NP-40, 1 mM EDTA, and 5% glycerol). Then, 100 µg of the total protein lysates were loaded onto a mini SDS-PAGE gel (4% stacking gel and 10% separating gel). The proteins were blotted onto nitrocellulose membrane using a semidry transfer system. The membrane was incubated with blocking solution for 30 minutes. The membrane was then incubated overnight with the primary antihuman PARP antibody and the β-actin antibody. The membrane was then incubated for three hours with the alkaline phosphate-conjugated secondary antibody, and the BCIP/NBT solution was used for the detection of the PARP and β-actin bands. The ImageJ software (1.44p National Institute of Health, USA) was used for the analysis of the intensities of the PARP protein band.

Examination of apoptotic DNA damage of the NCI-H209 cell line

The DNA damage was tested using the TUNEL assay (Invitrogen, mp2310, APO-BrdU™ TUNEL Assay Kit). First, 10^6 NCI-H209 small cell lung cancer cells (ATCC® HTB-172™) were incubated with ^{10}BDG in the growth medium (RPMI 1640 R8758-Sigma, 10% FCS, 0.5% Pen/Strep, Sigma-Aldrich). After three hours, the cells were collected and washed with PBS. The experimental procedure followed to detect DNA damage was the protocol recommended by the manual for the TUNEL assay kit.

Examination of apoptotic DNA damage of the NCI-H209 cell line

First, 25 x 10^4 cells were seeded in 6-well plates and treated with ^{10}BDG for three days. The conditioned media and trypsinized cells were placed in a 15-ml falcon tube and centrifuged at 1000 x g and RT for five minutes. The pellet was washed with cold PBS and centrifuged again at 1000 x g and RT for five minutes. The pellet was dissolved in 120 µl of lysis buffer (10 mM Tris pH 7.4, 100 mM NaCl, 25 mM EDTA, and 1% N-lauryl sarcosine) by gentle-vortexing and 4 µl of proteinase K (10 µg/µL) was then added. After the sample was incubated at 45°C for 2 h, 2 µl of RNAse (10 µg/ml) was added, and the cell lysates were incubated for one hour at room temperature. The lysate was run on a 2% agarose gel with N',N'-dimethyl-N-[4-[(E)-(3-methyl-1,3-benzothiazol-2-ylidene)methyl]-1-phenylquinolin-1-ium-2-yl]-N-propylpropane-1,3-diamine instead of ethidium bromide and 60 V for four hours. Caution was

taken during the loading process because the lysate was extremely sticky.

Proliferation assay of the NCI-H209 cell line

To examine the antiproliferative properties of ^{10}BDG and its additive effect with antineoplastic drugs (AMD), the MTT proliferation assay was applied. Cells of the NCI-H209 small lung cancer cell line were incubated with/without 20 mM ^{10}BDG and 2.5 mM AMD for 72 hours. At the end of the ^{10}BDG incubation (at the indicated times), 1/10 MTT solution was added to the cells, and the cells were incubated for one hour in a CO_2 incubator. The RPMI medium was removed with a centrifuge, and the purple MTT-formazan crystals were dissolved through the addition of 100 µl of DMSO. The purple colour was read at 570 nm using a microplate reader (Thermo Multiskan EX, Shanghai-China).

Examination of genotoxicity with plasmid DNA damage assay

250 ng of plasmid DNA (''8454 pCMV-VSV-G'') and ^{10}BDG (0, 20, 40, 80, and 160 µM) were added to a tube containing 2 µl of resuspended DNAse inactivation reagent (Ambion, AM1906). The mixtures were adjusted with double distilled H_2O to obtain a final concentration of 20 µl. Those mixtures were mixed well and centrifuged at an acceleration of 11,000 g, incubated at room temperature for 1.5 minutes and the contents were then transferred to another tubes and incubated for 24 hours and one week at 37°C. The reaction mixtures were loaded into a 1% agarose gel containing 0.5 µg/ml of ethidium bromide (Et-Br). 20 cm long gels were run at 6 V/cm for two hours.

Bearing tumor tissue in Copenhagen Rats (MAT-LyLu cell line)

Copenhagen Rat tumor model with MAT-LyLu cell line implantation is very useful for biodistribution and drug target studies [18]. Cancer tissue formation was induced by injection of $1x10^6$ MAT-LyLu cells into the left peritoneum of Copenhagen Rats, to examine whether 2-DG has carrier properties for ^{10}B to cancer tissue (MAT-LyLu: Rat prostate Adenocarcinoma cell line was a kind gift from Prof. Dr. Seyhan Altun, İstanbul University: ATCC JHU-92). Copenhagen Rats were anesthetized by the ketamine injection (100 mg/kg) previous to the cell injection. An average tumor size of 1 cm was achieved in seven days.

Biodistribution of ^{10}B in the tumor tissue

At the seventh day, tumor induced rats were subjected to diet for four hours and anesthetized by using ketamine (200 mg/kg) previous ^{10}BDG injection. Boric Acid ($B(OH)_3$) and/or ^{10}BDG solution were administrated to the rats having a body mass of 150 g via tail vein (^{10}B 30 mg/kg). Indicated tissues (Brain, Lung, Liver, Blood, Colon) including tumor tissue were taken after 40 minutes from ^{10}BDG injection under anesthesia. The tissues were homogenized by mechanical and ultrasonic homogenization. Samples were assayed by inductively coupled plasma atomic emission spectroscopy (ICP-AES, OPTIMA 2000 DV, Perkin Elmer Instruments). ^{10}B analysis was carried out by the wavelength at 249.772 nm and 7Li analysis was also performed at 670.784 nm [19].

Statistical analysis

Each experiment was repeated at least four times, and the results of a representative experiment are shown. The T test was applied to the variables, and each result is reported as the mean ± Standard Error of Mean (S.E.M). Statistical significance was accepted at P values of less than 0.05. Permission for the experimental animal study was obtained from the Yüzüncü Yıl University Experimental Animal Research Committee.

Results

Successful complexation reaction of boric acid and deoxy-D-glucose via a low-high pH reaction

In a previous complexation study, the polyhydroxyl compound Tiron (4,5-dihydroxy-1,3-benzenedisulfonic acid disodium salt) and boric acid were complexed using the low-high pH reaction described by Chaoying and coworkers, which was designed for the complexation of boric acid with deoxy-D-glucose (^{10}BDG). To demonstrate the complexation, FT-IR/ATR analyses were used to analyze the $^{10}B(OH)_3$-DG and $^{10}B(OH)_3$-Tiron reactions, and the success of the complexations was proven (Figure 1a, 1b, 1c) [13].

Cytotoxicity of ^{10}BDG

The cytotoxic levels of synthesized ^{10}BDG were tested on different cancer cell lines (HT29, MCF-7, Raji and H209) using the MTT assay (Fig. 2), the absorbance at 570nm was determined by spectrotometry. The growth inhibition rate was calculated as follows: Growth inhibition rate (%) = (1- OD570 experiment/D570 control) ×100%.

The cytotoxicity values of ^{10}BDG after three and 24 hours were found to be very close to those reported in the literature for the cytotoxicity of $^{10}B(OH)_3$ (Table 1, Fig. 2).

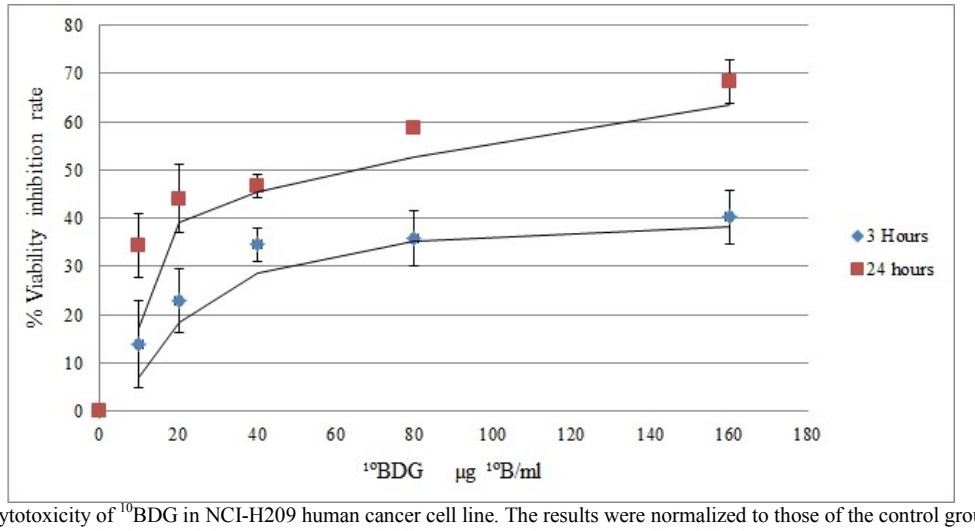

Figure 2: Cytotoxicity of ^{10}BDG in NCI-H209 human cancer cell line. The results were normalized to those of the control group (n = 5). The bars represent standard error of the mean. Exponential lines represent least-squares fits of the data.

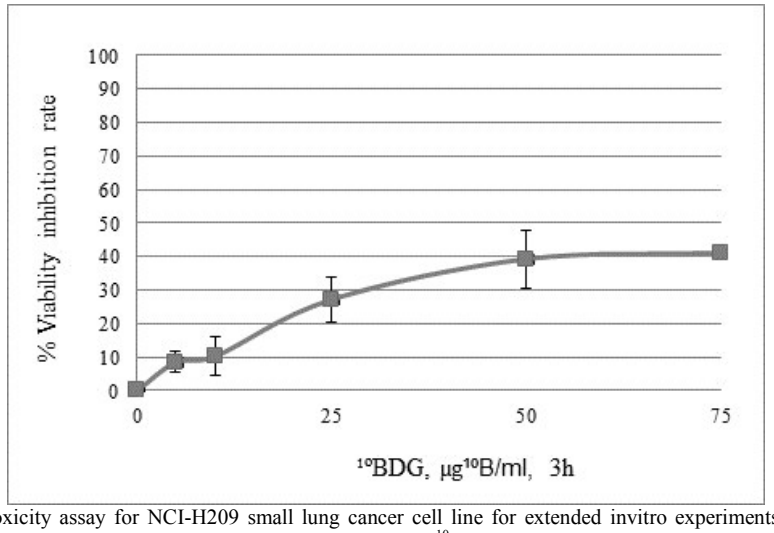

Figure 3: MTT cytotoxicity assay for NCI-H209 small lung cancer cell line for extended invitro experiments (Caspase activations, PARP cleavage, DNA damage TUNEL assay). Cells were incubated with ^{10}BDG for 3 hours. The bars represent the standard error of the mean (n = 5).

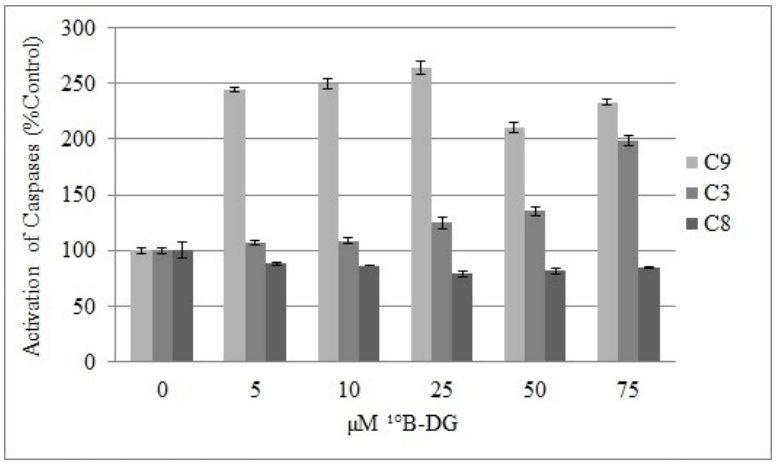

Figure 4: Flow cytometry analysis for activation of Caspase 3, 8, 9 (C3, C8, C9). NCI-H209 small lung cancer cells were induced to apoptosis by ^{10}BDG for 3 hours. The bars represent the standard error of the mean (n = 3). Activation of C3 and C9 was observed with increasing concentration of ^{10}BDG.

Evaluation of apoptotic pathway triggered by ^{10}BDG

The main two caspase streams (caspase-8 and caspase-9) were studied on NCI-H209 cell line. It is known that caspase-3 may be activated by both caspase-9 and caspase-8. In the present study, ^{10}BDG-induced caspase-9-dependent caspase-3 activation was observed (Figs. 3 and 4). These findings suggest that ^{10}BDG can trigger the mitochondrial apoptotic pathway and that the targeted cells can be destroyed through the apoptotic mechanism.

PARP cleavage determination

Poly ADP ribose polymerase (PARP) is an enzyme between the caspase stream and DNA ligases which cleavage of PARP results in DNA fragmentation. Also, PARP cleavage indicates the activation of the apoptosis mechanism, and western blot analyses revealed that ^{10}BDG induced PARP cleavages in H209 small cell lung cancer cells (ATCC® HTB-172™; Figs. 5 and 6) in a dose-dependent manner.

Examination of apoptotic DNA damage through flow cytometer

The activation of the caspase stream and PARP should result in DNA fragmentation. To examine the DNA fragmentation, the TUNEL assay and the DNA fragmentation agarose gel assay were used. These assays revealed that ^{10}BDG-induced DNA fragmentation was present in NCI-H209 small lung cell carcinoma cells in a dose-dependent manner (Figs. 7 and 8).

Proliferation assay

The inhibition of proliferation is the main target of antineoplastic drugs [20] (Shapiro et al., 1999). To analyze the effects of ^{10}BDG on proliferation, NCI-H209 small lung carcinoma cells were used. Actinomycin D (ActD) inhibits DNA-dependent RNA polymerases, may also induce apoptosis at high concentrations [21](Fraschini et al., 2005), and inhibits proliferation [22](Xu and Krystal, 2010). Even it does not seem to be statistically significant, the simultaneous exposure of H209 cells to ^{10}BDG and ActD demonstrates that ^{10}BDG may act synergistically with chemotherapeutics such as ActD and more effective results may be obtained with low dose chemotherapeutics (Fig. 9).

Examination of genotoxicity with plasmid DNA damage assay

Genotoxins/Carcinogens are a broader category of substances that induce DNA damage and changes to the structure or number of genes via chemical interaction with DNA. It is obvious that any synthesized molecules with therapeutic aims should not be genotoxic. To define the genotoxic/carcinogenic properties of ^{10}BDG, the plasmid DNA fragmentation assay was used. The results revealed that ^{10}BDG did not induce any plasmid DNA fragmentation, as determined through agarose gel affinity chromatography (Fig. 8). In contrast, the previous analyses had revealed that ^{10}BDG induced DNA fragmentation in NCI-H209 cells. Based on these two results (Figs. 8, 10), ^{10}BDG does not have genotoxicity but does exhibit apoptotic properties. Thus, ^{10}BDG looks appropriate for *in vivo* BNCT applications (Fig. 10). Tumor selective cytotoxic biological compounds may be a useful approach to avoid cumulative side effects of concomitant use of chemotherapeutics.

Build-up Tumor Tissue in Copenhagen Rats

To examine whether 2-DG has carrier properties for ^{10}B to cancer tissue, cancer tissue formation was induced with injections of MAT-LyLu cells to the left peritoneal of Copenhagen Rats. Copenhagen Rats were anesthetized by ketamine (100 mg/kg) before cell injection. It was observed that the induced tumors were about 1 cm in diameter after seven days.

Biodistribution of ^{10}B

The ICP-OES results demonstrate that the boron content of different tissues and blood was about 5 ppm in the all tissues and in the tumor of the control group (Fig. 11). Forty minutes after injection of 30 mg^{10}B/kg $^{10}B(OH)_3$, boron concentrations (^{10}B) in Brain, Colon, Liver, Lung, Blood and Tumor were 8.25, 8.98, 8.65, 9.09, 8.49 and 8.11 ppm, respectively. In contrast, 40 minutes after injection of 30 mg^{10}B/kg ^{10}BDG the boron concentration in Brain, Colon, Liver, Lung, Blood and Tumor were 8.02, 8.4, 8.17, 8.21, 7.62 and 12.63 ppm, respectively. Thus, in the tumor tissue the boron concentration was elevated to 12.63 ppm from 4.44 ppm, 40 minutes after ^{10}BDG injection (Fig. 11).

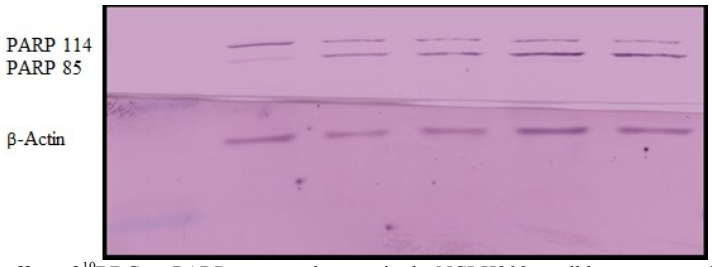

Figure 5: Dose-dependent effect of ^{10}BDG on PARP enzyme cleavage in the NCI-H209 small lung cancer cell line. Cells were exposed to various concentrations of ^{10}BDG for 3 hours and western blot analysis was applied. The poly(ADP-ribose) polymerase 114 kDa nuclear enzyme (PARP114), is cleaved in main fragments of 85 kDa during apoptosis (PARP85). The housekeeping protein β-Actin was used as a loading control.

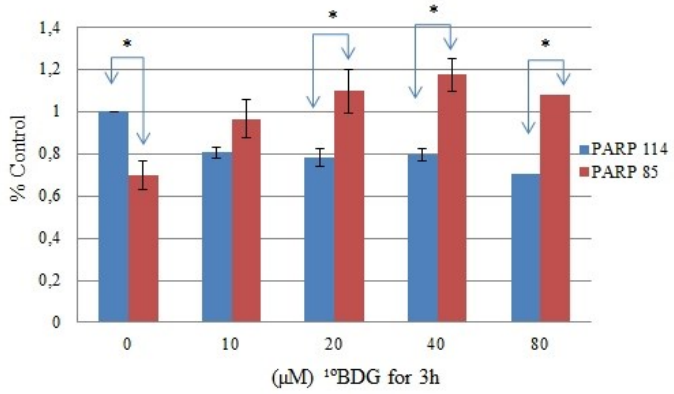

Figure 6: Analysis of dose-dependent effect of ^{10}BDG on PARP enzyme cleavage in the NCI-H209 small lung cancer cell line. The bars represent the standard error of the mean (n = 3); * indicates a statistically significant difference between the band intensities of the compared groups ($P \leq 0.05$).

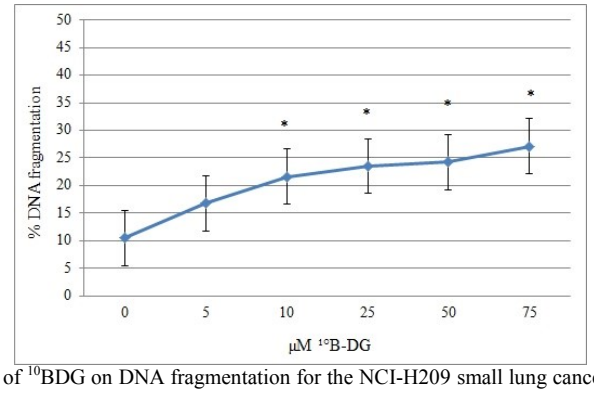

Figure 7: Dose depended effect of ^{10}BDG on DNA fragmentation for the NCI-H209 small lung cancer cell line. The bars represent the standard error of the mean (n=3) (* $P \leq 0.05$).

Discussion

Since the 1960s, researchers have exhibited a growing interest in BNCT due to the increase of cancer incidence worldwide. The success of BNCT depends on two factors [23]: (1) neutron production at an appropriate dose and energy and (2) delivery of sufficient amounts of ^{10}B specifically to the tumor tissue [24].

So far, a wide variety of boron delivery agents have been synthesized [25] and tested, but only two drugs (BSH and BPA) have been used in clinical trials: Since 1968, a polyhedral borane anion, which is known as sodium borocaptate or BSH ($Na_2B_{12}H_{11}SH$), has been used in Japan [26]. To plan an improved radiation therapy, boron phenylalanine (BPA), which is a dihydroxyboryl derivative of phenylalanine, with or without mannitol was used for the treatment of patients with glioblastoma [27].

The use of boric acid supplements is another approach to preparation of the patients for BNCT. *In vivo* epidemiologic studies have shown that boron and boric acid affect human health. As defined previously, 98.4% of the boron in the blood is found in the form of boric acid [28]. According to several studies, the supplementation of food with boron reduces the risk of some cancers [29, 30]. Moreover, Gallardo-Williams et al. showed that additional boron taken with food reduces the size of tumors and the level of IGF-I in rats [31].

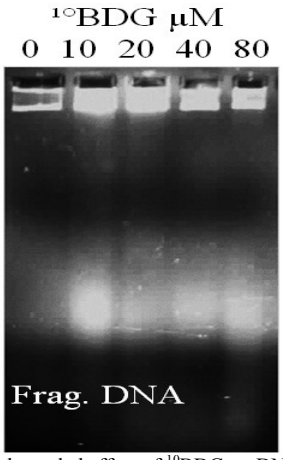

Figure 8: Representative Agarose gel image; Dose depended effect of ^{10}BDG on DNA fragmentation in the NCI-H209 small lung cancer cell line

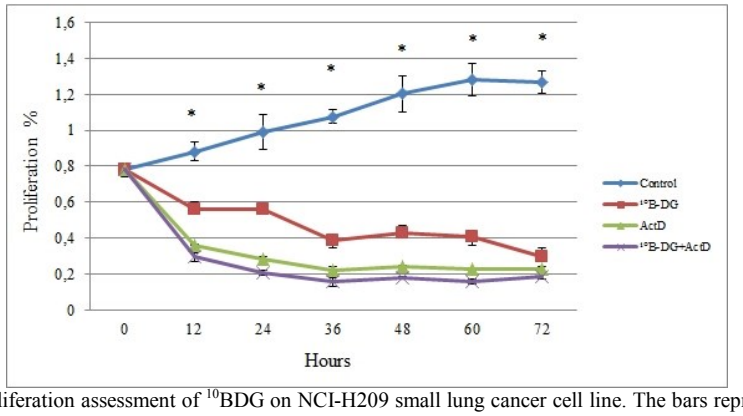

Figure 9: MTT cell proliferation assessment of ^{10}BDG on NCI-H209 small lung cancer cell line. The bars represent the standard error of the mean (n = 4). * indicates statistically significant differences between the Control groups and those treated with ^{10}BDG or ActD (* $P \leq 0.05$).

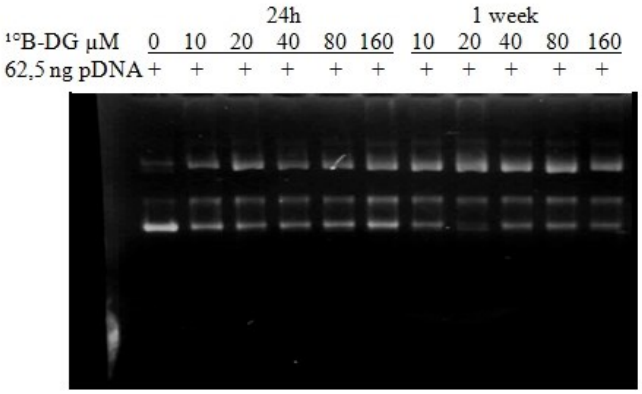

Fig 10 Agarose gel electrophorese image of plasmid DNA genotoxicity assay.

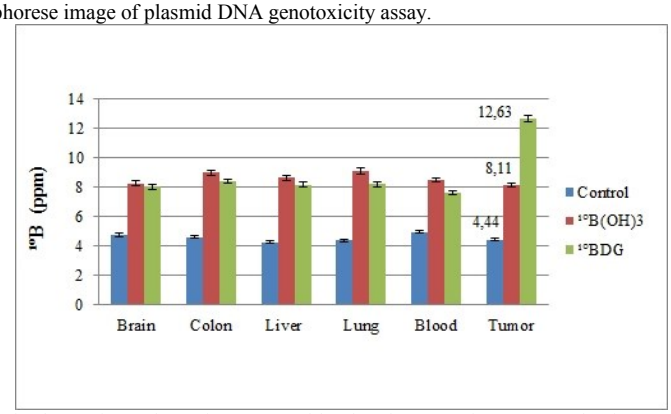

Fig 11 Boron concentration in the Brain, Colon, Liver, Lung, blood and Tumor tissue assayed using ICP-OES. Administered dose of boron was 30mg ^{10}B/kg. The results correspond to mean values of 3 animals. The bars represent the standard error of the mean

Table 1. Inhibitory concentration 50 (IC_{50}: 50% growth-inhibitory effect) MTT assay results of ^{10}B-DG *in vitro* and calculation of lethal dose 50 (LD_{50}) from IC_{50}. The IC_{50} values were obtained from dose-response curves after fitting the data (GraphPad Prism 6.03-log(inhibitor) vs. normalized response - Variable slope) (Mean±SD, n≥3)

		*LogIC$_{50}$	LogLD$_{50}$ (mg/kg)
MCF-7	3h	133±13	51,5±7
	24h	93,7±11	36,9±6
HT29	3h	131,9±26	51,4±12
	24h	79±9	31,7±5
RAJI	3h	121,2±18	47,1±9
	24h	129,6±8	50,2±5
H209	3h	180±32	69,0±14
	24h	72,1±10	28,8±6

*Best-fit values ± Std. Error
LogLD50 (mg/kg) = 0.372 logIC50 (ug/mL)+2.024

Acerbo and Miller reported that boron prevents the proliferation of cancer cells in melanoma [32]. Henderson and co-workers confirmed that a high level of boric acid in the blood reduces the risk of prostate cancer by reducing the level of Ca^{++} in cells and signal transmission [33]. Scorei and co-workers demonstrated the antiproliferative effects of boric acid and calcium fructoborate (the form of boron in food) in breast cancer cells and also showed that calcium fructoborate induces apoptosis [34]. Hsu and co-workers showed that boric acid may be helpful for the treatment of bone cancers because it has cytotoxic effects and it accumulates in bones [19].

An increasing number of successful results have been found for boric acid and BNCT in clinical trials. For instance, Wang et al. showed that BNCT treatment has positive effects on head and neck cancers and that the lifespan of a patient may be extended with BNCT [35]. In phase I and phase II studies, a significant reduction in the size of the tumor was confirmed in all patients, and the side effects were evaluated as tolerable. In addition to BNCT alone, the synergistic effects of BNCT with classic radiation treatment in glioblastoma are being studied in phase II studies. [36, 37].

Boron targeting to tumor tissue is an important problem and likely the most important challenge associated with BNCT. To solve this problem, different carrier molecules have been used to increase the rate of boric acid passing into cancer cells and to minimize the damage to normal cells. Porphyrin [38], polyamines based on polylysine [39], and fructose [40] are some of molecules that increase the selectivity and anticarcinogenic effects of boron.

Although boron has some effects on tumorigenic tissues and cells, it has no tumor-selective properties and is thus not convenient for BNCT applications. Thus, the research priority for BNCT is to synthesize tumor-selective boron. Large-scale boron carriers, such as carborane-containing porphyrins and cholesterol-metallacarboranes bearing cobalt, iron, and chromium, were designed and tested in previous studies [41, 42].

The main two challenges associated with the identification of appropriate carriers are the toxicity of the newly synthesized molecules and the carrier properties of boron to tumor tissue. The evaluation of the accumulation of boron in different tissues demonstrates that liver toxicity is the problem that is most encountered by the tested carriers [41, 42].

2-Deoxy-d-glucose contains poly-hydroxyl compounds, and its complexation with boric acid (^{10}BDG**)** was achieved in the present study through a pH reaction, as previously described for boric acid complexation with poly-hydroxyl compounds [13].

In the present study, cytotoxic levels of ^{10}BDG were evaluated on different cancer cell lines, and it was found that ^{10}BDG triggered the activation of the apoptotic pathway that involves caspase 9 and caspase 3. Western blot analysis revealed PARP cleavage, and the TUNEL assay and flow cytometer were used to demonstrate the existence of protolytic DNA damage caused by PARP-induced DNA ligase**.**

It is known that the most significant feature of tumor tissue is uncontrolled excessive mitosis and ATP requirements. An increase in the tumor tissue biomass also increases the energy needs and decreases the oxygen supplies. Consequently, the required ATP is produced through anaerobic pathways [11]. The yield of the anaerobic synthesis of ATP is very low and leads to an increased glucose consumption rate [43].

Due to the affinity of glucose to tumor tissue, glucose-complexed drugs are currently an intensive interest area for antineoplastic drug studies. In the present study, a type of glucose derivative (2-DG) was used as boron carrier to selectively target tumor tissue.

For biodistrubition studies in the experimental animal model, boron dose application varies between 25-50 mg^{10}B/kg in different studies [19]. IC_{50}, IC_1 and calculated LD_{50}, LD_1 values may be useful to calculate optimum non-toxic application dose for biodistribution studies on rats; however, further in vivo investigations are needed to define maximum applicable doses before proceeding to clinical applications.

Hsu and co-workers recommend use of boric acid for osteosarcoma tumors. However, in the present study, tumor selectivity of boric acid was not observed for both soft tissues and adenocarcinoma metastatic prostate tumor tissue. The results obtained in the present study on the control group support the findings of Hsu and co-workers [19].

Literature findings suggest that the boron concentration in tumor tissue must be 15-30 ppm, for BNCT application. In the present study, the measured boron concentration was elevated to 12.8 ppm (about 2.8 times increase) in the tumor tissue by the ^{10}BDG injection. Extended infusion time may increase accumulation of boron to 15-30 ppm in the tumor tissue.

Beside biodistribution time-lapse analysis, a synergistic use of different boron carriers such as the simultaneous use of glucose derivative and essential amino acid carriers to achieve the required boron concentration in the tumor tissue could be another strategy to avoid the toxic effect of boron carriers.

Moreover cytotoxicity, genotoxicity and apoptotic pathway studies were performed. No genotoxicity was observed and the cytotoxic mechanism was the caspase-dependent apoptotic pathway. While anti-proliferative properties, induction of apoptosis, etc. would be beneficial, cytotoxicity over the normal tissue is restricting use of new synthesized ^{10}B carriers. According to the present results, ^{10}BDG has relatively low cytotoxic values (i.e., the LD50 value is on average 537.50 μM) if compared with chemotherapeutics such as AMD; therefore it seems worth to continue to work on this.

Considering the apoptotic and antiproliferative properties of ^{10}BDG and the carrier properties of DG, ^{10}BDG and ^{10}B^{18}FDG, these complexes can be an alternative boron carrier in lieu of boronophenylalanine (BPA) and BSH for BNCT. Consequently, BNCT studies with ^{10}BDG are currently being performed at the TRIGA MARKII Nuclear Reactor of the Energy Institute at Istanbul Technical University.

Acknowledgments

This research was supported by grants from the Turkey National Boron Research Institute (BOREN-2011-Ç0289). The authors thank Drs. Aysın Tolunay, Ertuğrul Yalçın, and Yusuf Kemal Demir, Marmara University Experimental Animal Research Center (DEHAMER), and Prof. Dr. Seyhan Altın Istanbul University, Life Sciences Institute, Department of Molecular Biology and Genetics for their contributions.

Conflict of Interest: The authors declare no potential conflicts of interest with respect to the research, authorship, and/or publication of this article.

References

1. Uusi-Simola J, Savolainen S, Kangasmaki A, Heikkinen S, Perkio J, Abo Ramadan U, et al. Study of the relative dose-response of BANG-3 polymer gel dosimeters in epithermal neutron irradiation. Physics in medicine and biology. 2003;48(17):2895-906.

2. Farr LE, Sweet WH, Robertson JS, Foster CG, Locksley HB, Sutherland DL, et al. Neutron capture therapy with boron in the treatment of glioblastoma multiforme. The American journal of roentgenology, radium therapy, and nuclear medicine. 1954;71(2):279-93.

3. Hopewell JW, Morris GM, Schwint A, Coderre JA. The radiobiological principles of boron neutron capture therapy: a critical review. Applied radiation and isotopes : including data, instrumentation and methods for use in agriculture, industry and medicine. 2011;69(12):1756-9.

4. US EPA. Available: http://www.epa.gov/radiation/rert/radfacts.html Accessed 4 Jun 2013. 2012.

5. Werner-Wasik M, Yu X, Marks LB, Schultheiss TE. Normal-tissue toxicities of thoracic radiation therapy: esophagus, lung, and spinal cord as organs at risk. Hematology/oncology clinics of North America. 2004;18(1):131-60, x-xi.

6. Joensuu H, Kankaanranta L, Seppala T, Auterinen I, Kallio M, Kulvik M, et al. Boron neutron capture therapy of brain tumors: clinical trials at the finnish facility using boronophenylalanine. Journal of neuro-oncology. 2003;62(1-2):123-34.

7. Evangelista L, Jori G, Martini D, Sotti G. Boron neutron capture therapy and 18F-labelled borophenylalanine positron emission tomography: a critical and clinical overview of the literature. Applied radiation and isotopes : including data, instrumentation and methods for use in agriculture, industry and medicine. 2013;74:91-101.

8. Shukla S, Wu G, Chatterjee M, Yang W, Sekido M, Diop LA, et al. Synthesis and biological evaluation of folate receptor-targeted boronated PAMAM dendrimers as potential agents for neutron capture therapy. Bioconjugate chemistry. 2003;14(1):158-67.

9. Garabalino MA, Heber EM, Monti Hughes A, Gonzalez SJ, Molinari AJ, Pozzi EC, et al. Biodistribution of sodium borocaptate (BSH) for boron neutron capture therapy (BNCT) in an oral cancer model. Radiation and environmental biophysics. 2013;52(3):351-61.

10. Dwarakanath BS. Cytotoxicity, radiosensitization, and chemosensitization of tumor cells by 2-deoxy-D-glucose in vitro. Journal of cancer research and therapeutics. 2009;5 Suppl 1:S27-31.

11. Skoyum R, Eide K, Berg K, Rofstad EK. Energy metabolism in human melanoma cells under hypoxic and acidic conditions in vitro. British journal of cancer. 1997;76(4):421-8.

12. Akan Z, Demiroglu H, Avcibasi U, Oto G, Ozdemir H, Deniz S, Basak AS. Complexion of Boric Acid with 2-Deoxy-D-glucose (DG) as a novel boron carrier for BNCT. Journal of Medical Science and Discovery, October. 2014;1(3):65-71.

13. Chaoying S, Shiro M, Yoshinobu M, Kazuhisa Y. Studies on the Complexation of Boric Acid with Polyhydroxyl Compounds. Analytical Sciences. 2001;17.

14. Moss GP, Smith PAS, Tavernier D. Glossary of class names of organic compounds and reactivity intermediates based on structure (IUPAC Recommendations 1995). Pure Appl Chemistry. 1995; 67(8-9):1307-1375.

15. IUPAC. Provisional Recommendations,Preferred IUPAC Names, Chapter. 2004;6:Sec P-68.

16. Carter J. American Chemical Society, Inorganic. Chemistry. 1968;7 (10):1945–1964.

17. ICCVAM. Peer review panel report: the use of in vitro basal cytotoxicity test methods for estimating starting doses for acute oral systemic toxicity testing. NIH publication no: 07-4519. Research Triangle Park: National Toxicology Program Available. 2006; http://iccvam.niehs.nih.gov/methods/acutetox/inv_nru_tmer.htm Accessed 4 June 2013.

18. Jiang J, Kulp SK, Sugimoto Y, Liu S, Lin YC. The effects of gossypol on the invasiveness of MAT-LyLu cells and MAT-LyLu cells from the metastasized lungs of MAT-LyLu-bearing Copenhagen rats. Anticancer research. 2000;20(6B):4591-7.

19. Hsu CF, Lin SY, Peir JJ, Liao JW, Lin YC, Chou FI. Potential of using boric acid as a boron drug for boron neutron capture therapy for osteosarcoma. Applied radiation and isotopes : including data, instrumentation and methods for use in agriculture, industry and medicine. 2011;69(12):1782-5.

20. Shapiro GI, Harper JW. Anticancer drug targets: cell cycle and checkpoint control. The Journal of clinical investigation. 1999;104(12):1645-53.

21. Fraschini A, Bottone MG, Scovassi AI, Denegri M, Risueno MC, Testillano PS, et al. Changes in extranucleolar transcription during actinomycin D-induced apoptosis. Histology and histopathology. 2005;20(1):107-17.

22. Xu H, Krystal GW. Actinomycin D decreases Mcl-1 expression and acts synergistically with ABT-737 against small cell lung cancer cell lines. Clinical cancer research : an official journal of the American Association for Cancer Research. 2010;16(17):4392-400.

23. Capuani S, Porcari P, Fasano F, Campanella R, Maraviglia B. 10B-editing 1H-detection and 19F MRI strategies to optimize boron neutron capture therapy. Magnetic resonance imaging. 2008;26(7):987-93.

24. Barth RF, Soloway AH, Fairchild RG, Brugger RM. Boron neutron capture therapy for cancer. Realities and prospects. Cancer. 1992;70(12):2995-3007.

25. Renner MW, Miura M, Easson MW, Vicente MG. Recent progress in the syntheses and biological evaluation of boronated porphyrins for boron neutron-capture therapy. Anti-cancer agents in medicinal chemistry. 2006;6(2):145-57.

26. Gibson CR, Staubus AE, Barth RF, Yang W, Ferketich AK, Moeschberger MM. Pharmacokinetics of sodium borocaptate: a critical assessment of dosing paradigms for boron neutron capture therapy. Journal of neuro-oncology. 2003;62(1-2):157-69.

27. Cruickshank GS, Ngoga D, Detta A, Green S, James ND, Wojnecki C, et al. A cancer research UK pharmacokinetic study of BPA-mannitol in patients with high grade glioma to optimise uptake parameters for clinical trials of BNCT. Applied radiation and isotopes : including data, instrumentation and methods for use in agriculture, industry and medicine. 2009;67(7-8 Suppl):S31-3.

28. Sutherland B, Strong P, King JC. Determining human dietary requirements for boron. Biological trace element research. 1998;66(1-3):193-204.

29. Barranco WT, Eckhert CD. Cellular changes in boric acid-treated DU-145 prostate cancer cells. British journal of cancer. 2006;94(6):884-90.

30. Cui Y, Winton MI, Zhang ZF, Rainey C, Marshall J, De Kernion JB, et al. Dietary boron intake and prostate cancer risk. Oncology reports. 2004;11(4):887-92.

31. Gallardo-Williams MT, Chapin RE, King PE, Moser GJ, Goldsworthy TL, Morrison JP, et al. Boron supplementation inhibits the growth and local expression of IGF-1 in human prostate adenocarcinoma (LNCaP) tumors in nude mice. Toxicologic pathology. 2004;32(1):73-8.

32. Acerbo AS, Miller LM. Assessment of the chemical changes induced in human melanoma cells by boric acid treatment using infrared imaging. The Analyst. 2009;134(8):1669-74.

33. Henderson K, Stella SL, Kobylewski S, Eckhert CD. Receptor activated Ca(2+) release is inhibited by boric acid in prostate cancer cells. PloS one. 2009;4(6):e6009.

34. Scorei RI, Rotaru P. Calcium fructoborate--potential anti-inflammatory agent. Biological trace element research. 2011;143(3):1223-38.

35. Wang LW, Wang SJ, Chu PY, Ho CY, Jiang SH, Liu YW, et al. BNCT for locally recurrent head and neck cancer: preliminary clinical experience from a phase I/II trial at Tsing Hua Open-Pool Reactor. Applied radiation and isotopes : including data, instrumentation and methods for use in agriculture, industry and medicine. 2011;69(12):1803-6

36. Hopewell JW, Gorlia T, Pellettieri L, Giusti V, B HS, Skold K. Boron neutron capture therapy for newly diagnosed glioblastoma multiforme: an assessment of clinical potential. Applied radiation and isotopes : including data, instrumentation and methods for use in agriculture, industry and medicine. 2011;69(12):1737-40.

37. Kawabata S, Miyatake S, Hiramatsu R, Hirota Y, Miyata S, Takekita Y, et al. Phase II clinical study of boron neutron capture therapy combined with X-ray radiotherapy/temozolomide in patients with newly diagnosed glioblastoma multiforme--study design and current status report. Applied radiation and isotopes : including data, instrumentation and methods for use in agriculture, industry and medicine. 2011;69(12):1796-9.

38. Evstigneeva RP, Zaitsev AV, Luzgina VN, Ol' Shevskaya VA, Shtil AA. Carboranylporphyrins for boron neutron capture therapy of cancer. Current medicinal chemistry Anti-cancer agents. 2003;3(6):383-92.

39. Umano M, Uechi K, Uriuda T, Murayama S, Azuma H, Shinohara A, et al. Tumor accumulation of epsilon-poly-lysines-based polyamines conjugated with boron clusters. Applied radiation and isotopes : including data, instrumentation and methods for use in agriculture, industry and medicine. 2011;69(12):1765-7.

40. Andoh T, Fujimoto T, Sudo T, Fujita I, Imabori M, Moritake H, et al. Boron neutron capture therapy for clear cell sarcoma (CCS): biodistribution study of p-borono-L-phenylalanine in CCS-bearing animal models. Applied radiation and isotopes : including data, instrumentation and methods for use in agriculture, industry and medicine. 2011;69(12):1721-4.

41. Kreimann EL, Miura M, Itoiz ME, Heber E, Garavaglia RN, Batistoni D, et al. Biodistribution of a carborane-containing porphyrin as a targeting agent for Boron Neutron Capture Therapy of oral cancer in the hamster cheek pouch. Archives of oral biology. 2003;48(3):223-32.

42. Bialek-Pietras M, Olejniczak AB, Tachikawa S, Nakamura H, Lesnikowski ZJ. Towards new boron carriers for boron neutron capture therapy: metallacarboranes bearing cobalt, iron and chromium and their cholesterol conjugates. Bioorganic & medicinal chemistry. 2013;21(5):1136-42.

43. Gonzalez MJ, Miranda Massari JR, Duconge J, Riordan NH, Ichim T, Quintero-Del-Rio AI, et al. The bio-energetic theory of carcinogenesis. Medical hypotheses. 2012;79(4):433-9.